Removal of Copper Ions from Wastewater Using Magnetite Loaded On Active Carbon (AC) and Oxidized Active Carbon (OAC) Support

Aya S. Mahmoud[a] , Nadia A.Youssef[a], Ahmed O. Abo El Naga[b], M.M.Selim[c]

a. Faculty of Women Ain Shams University.
b. Egyptian Petroleum Research Institute (EPRI).
c. National Research Centre (NRC).

Abstract:

The magnetite Fe_3O_4 was supported on active carbon AC (Fe_3O_4 /AC) and oxidized active carbon OAC (Fe_3O_4 /OAC). It was prepared by co-precipitation method and characterized by X-ray diffraction (XRD), scanning electron microscope (SEM), surface area measurements (BET) and vibrating sample magnetometer (VSM) techniques. Fe_3O_4 /AC and Fe_3O_4 /OAC were used as adsorbents for removal of Cu (II) ions from wastewater. The effect of adsorption parameters such as contact time, the pH of the solution, the weight of adsorbent and the initial concentration of Cu(II) ions was elucidated to achieve the process's optimal operational conditions. It was found that the removal percentage of the Cu(II) ions was reached to 96.15 % after 30 min. The adsorption process fitted very well the pseudo-second-order model and the adsorption equilibrium data could be well described by the Langmuir isotherm.

1.Introduction:

The effluents carrying high concentration of heavy metals are extremely toxic to human and aquatic life; resulting in kidney and liver problems and genotoxic carcinogen, ultimately deteriorating public human health ***[Muhammad et al ., 2011],[Luo et al.,2016]***. The main source of heavy metals polluting the drinking water is the industrial wastewater (produced primarily in modern chemical industries based on fossil fuels, batteries, metal plating, pesticides, and many others) ***[Ihsanullah et al.,2016].*** Though many metals are prerequisite in small quantities for good health, but they may be toxic for human at high level like copper ***[Randhaw et al.,2015]***. The presence of copper ions are believed to severely poison the drinking water ***[Fu and Wang 2011]***. The excessive ingestion of Cu(II) ions causes numerous health issues including an increased blood pressure and respiratory variations (causing serious damages within the kidney and liver), convulsion, cramps, vomiting, or even death ***[Ihsanullah et al.,2016],[Si-Yong et al., 2019].***

***Corresponding author:** aya.s.ibrahem90@gmail.com.

To alleviate these undesired consequences, many techniques have been devoted for removing metal ions including bioremediation, coagulation, lime softening, chemical precipitation, membrane filtration, solvent extraction, electrolysis, reverse osmosis, ion exchange and adsorption ***[Awual et al.,2013], [Liu et al., 2008], [Babel and Kurniawan 2003], [Perić et al., 2004].***

Among various techniques, adsorption is considered the most promising one used in the removal of toxic metals adopting nanomaterials as nanosorbents ***[Friedrich et al.,1998],[Dimitrov et al., 2006],[Nikhat and Weqar 2015].***

The removal of heavy metals via sorption techniques has to achieve discharge standards, a low maintenance and operation cost and low energy efficiency ***[Ming et al.,2012].*** Activated carbons are mostly used in adsorption of wide variety of water pollutants or in water treatment because of its ability to improve water by removing toxic materials ***[Babak et al.,2014].***

Iron oxide nano materials have special advantage in water purification technology due to its super paramagnetic property, least toxicity, biodegradablility, environmental friendly, easy and facile synthesis etc. ***[Huang et al., 2003], [Gupta et al., 2005].***

Recently, magnetic activated carbon particles (MACP) have received considerable attention due to their high surface area and superior magnetic properties as an emerging adsorbent ***[Si-Yong et al., 2019]***. The main objective of the present work is to verify the successful application of synthesized magnetite Fe_3O_4loaded on active carbon support AC (Fe_3O_4 /AC) and oxidized active carbon support OAC (Fe_3O_4 /OAC) as adsorbents for the removal of Cu(II) ions from wastewater.

2.1.Materials (chemicals).

Ferrous Chloride ($FeCl_2$), Ferric chlorid ($FeCl_3.6H_2O$), Copper nitrate $Cu(NO_3)_2.5H_2O$, were provided from LOBA Chemic, Ammonium hydroxide NH_4OH 33%, commercial active carbon (AC) powders and Nitric acid (HNO_3) were supplied by laboratory Rasayan. All the chemicals were of analytical grade and were used without further purification.

2.2 Methods:

2.2.1. Preparation of adsorbent:

- **Preparation of oxidized active carbon (OAC) support :**

Oxidized active carbon (OAC) support was prepared by weighing 15 gm of active carbon (AC) which was oxidized by impregnating the particles with concentrated HNO_3 and heating at 95° C for two hours with vigorous stirring.

- **Preparation of magnetite nanoparticles:**

Magnetite nanoparticles were prepared by co-precipitation method as reported earlier ***[Roto et al.,2016], [Binu et al.,2011].*** This method seems to be promising because of its simplicity and productivity. $FeCl_3.6H_2O$ and $FeCl_2.4H_2O$ were dissolved in a 2:1 molar ratio in distilled water with stirring under nitrogen and this solution which contains both Fe ions was then heated up to 80° C. After heating, ammonium hydroxide was added drop-wise to raise the pH up to 8.0 with continuous stirring at 80° C for 30 minute. At this pH the solution turned from brown to black. Subsequently, black particles were separated and quickly washed three times with distilled water. The magnetite was then dried in hot air oven at 100° C for 24 hours ***[Binu et al.,2011],[Shalini et al.,2016].***

- **Preparation of a series of Fe_3O_4 supported on active carbon (Fe_3O_4/AC) and on oxidized active carbon (Fe_3O_4/AC) with different ratios of Fe_3O_4:**

Active carbon (AC) and oxidized active carbon (OAC) supports were simply added into the mixed solution of ferric chloride and ferrous chloride with stirring under nitrogen before the addition of ammonia solution. The process followed the same steps as the preparation of Fe_3O_4. The magnetite was supported on (AC) at different ratios of Fe_3O_4, viz., 7.5 wt% ,15 wt% and 30 wt % Fe_3O_4/AC. The best ratio of Fe_3O_4/AC was selected to be compared with the same ratio of Fe_3O_4/OAC.

2.2.2. Preparation of copper ion solution (adsorbate):

A stock solution of Cu(II) (1000 mg/l) was prepared. Different concentrations of Cu(II) ranging between 50 mg/l and 500 mg/l were prepared by dilution from this stock by distilled water, to be utilized for adsorption experiments.

2.2.3. Adsorption of copper ions:

Batch adsorption experiments of the Cu(II) ions by Fe_3O_4/AC and Fe_3O_4/OAC adsorbents were carried out at room temperature by shaking a series of bottles each contains the desired quantity of the adsorbent in a predetermined concentration of copper ion solutions. Samples were withdrawn at different time intervals; the supernatant was separated and analyzed for remaining heavy metal content. The percent removal of heavy metal from solution was calculated by the following equation ***[Long et al.,2016]:***

$$\% \text{ Adsorption} = \frac{C_o - C_e}{C_o} \times 100$$

Where; C_o is initial concentration of heavy metal, C_e is final concentration of heavy metal.

2.2.4. Adsorption isotherms:

The adsorption isotherm that describes the adsorption pattern between the Cu(II) adsorbed metal ions on the adsorbent and the residual metal ions in the solution during the surface adsorption was conducted. Equilibrium isotherms were measured to determine the capacity of the adsorbent for metal ions. The most common types of models describing this type of system are the Langmuir and Freundlich models ***[Shamsan et al.,2018].*** The adsorption capacity q_e (mg/g) after equilibrium was calculated by a mass balance relationship equation as follows:

$$q_e = (C_o - C_e)\frac{V}{W}$$

Where C_o is the initial and C_e is the equilibrium concentrations of the test solution (mg/L), V is the volume of the solution (L) and W is the mass of adsorbent (g).

2.2.4.1. Langmuir model

Langmuir adsorption model is based on the assumption that the maximum adsorption corresponds to a saturated monolayer of solute molecules on the adsorbent surface. Langmuir equation can be described by the linearized form ***[Sekar et al., 2004], [Hameed et al., 2008]:***

$$\frac{1}{q_e} = \left(\frac{1}{q_m K_L}\right).\left(\frac{1}{C_e}\right) + \frac{1}{q_m}$$

Where, C_e is the equilibrium concentration of metal ions in solution (mg/L), $q_e$is the amount of metal ion adsorbed on adsorbents (mg/g), and $q_m$and K_L are the monolayer adsorption capacity (mg/g) and Langmuir equilibrium constant (L/mg) which indicates the nature of adsorption. The values of $q_m$and K_L were determined graphically. The plot of $\frac{1}{q_e}$ versus $\frac{1}{C_e}$, yields a straight line having slope equal to $\frac{1}{q_m K_L}$ and intercept $\frac{1}{q_m}$, which corresponds to complete monolayer coverage.

2.2.4.2. Freundlich model

Freundlich adsorption isotherm represents the relationship between the amount of metal adsorbed per unit mass of the adsorbent q_e and the concentration of the metal in solution at equilibrium. Freundlich equation can be described by the linearized form ***[Ertugay et al., 2014]:***

$$Log\ q_e = log\ K_F + {}^{1}\!/_{n}\ log\ C_e$$

where, k_F and n are Freundlich constants. The values of k_F and n were determined graphically. A plot of log q_e versus log C_e gives a straight line of a slope ${}^{1}\!/_{n}$ and the intercept

is logK_F. The value of K_F indicates the adsorption capacity while $1/n$ is indicative of the intensity of the reaction.

3. Results and discussion:

3.1. Characterization of adsorbent:

3.1.1.X-ray diffraction (XRD).

Purity and crystalline structures of AC and OAC supports, Fe_3O_4/AC, Fe_3O_4/OAC and Fe_3O_4 were examined using powder X-ray diffraction (XRD). Figure (1) shows broad diffraction peaks with 2Ɵ in the range about 20°-30° and 41°-46°, attributed to the (002), (100) and (101) crystallographic planes of porous carbon, (JCPDS, Card No. 75-1621), respectively ***[Wu et al., 2013], [Luaand Yang,2004],[Wang et al.,2014] and [Prahas et al.,2008]***. In this figure, the

diffraction peaks of Fe_3O_4 corresponding to (220), (311), (400), (511), and (440) planes, occurred at 2θ = 30.1°, 36.3°, 43.4°, 57.2°, and 62.3°, respectively, are quite identical to the cubic phase nanoparticles of Fe_3O_4 with a face centered cubic structure (JCPDS No. 89-3854) ***[Srivastava and Majumder,2008], [Si-Yong et al., 2019]***.

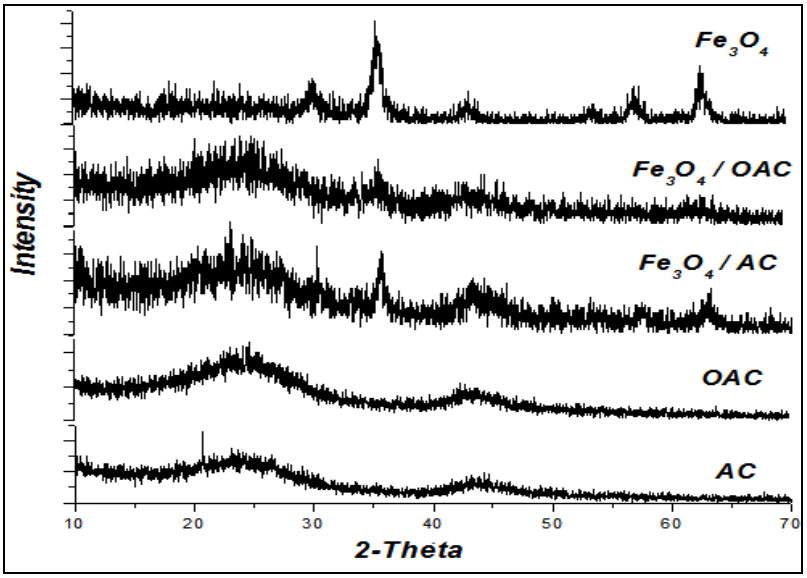

Fig.(1): X-ray diffraction patterns of AC and OAC support ,Fe_3O_4/AC, Fe_3O_4/OAC and Fe_3O_4.

3.1.2 Surface area measurements.

N_2 adsorption-desorption isotherms and pore size distribution curves of the porous (a) AC,(b) OAC, (c) Fe_3O_4 /AC and (d) Fe_3O_4 /OAC are shown in Fig. (2). All the samples presented a typical type I isotherms characteristic of microporous materials according to IUPAC classification of adsorption isotherms. The obtained Brunauer–Emmett–Teller (BET)

surface area were 1136, , 1002, 1147 and 961 m^2/g with average pore volumes 0.56,0.57,0.51, 0.49 cm^3/g of the AC, Fe_3O_4/AC, OAC and Fe_3O_4 /OAC respectively. As shown from these results OAC support seems having surface area greater than AC support; for both, the surface area decreased with the loading extent.

The pore size distribution was also calculated by using the original density functional theory (DFT) method. The DFT curve shows the pore diameter of all samples ranging from (1.0-1.13) nm, confirming the nanoporosity nature of the used samples

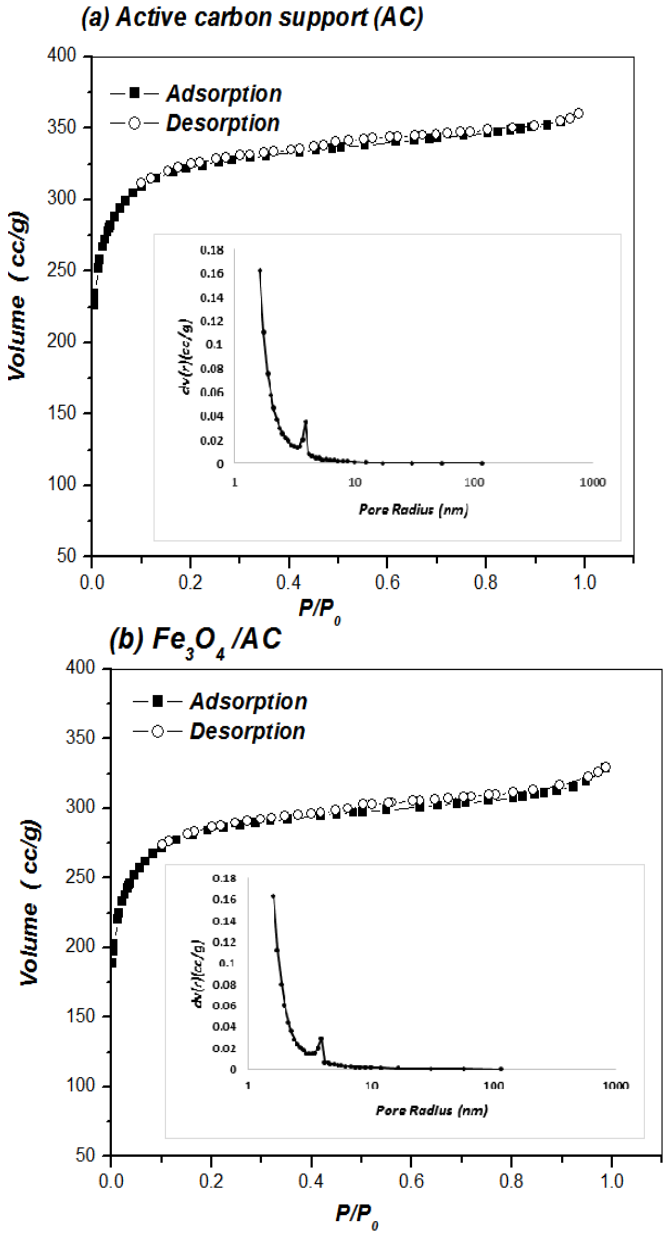

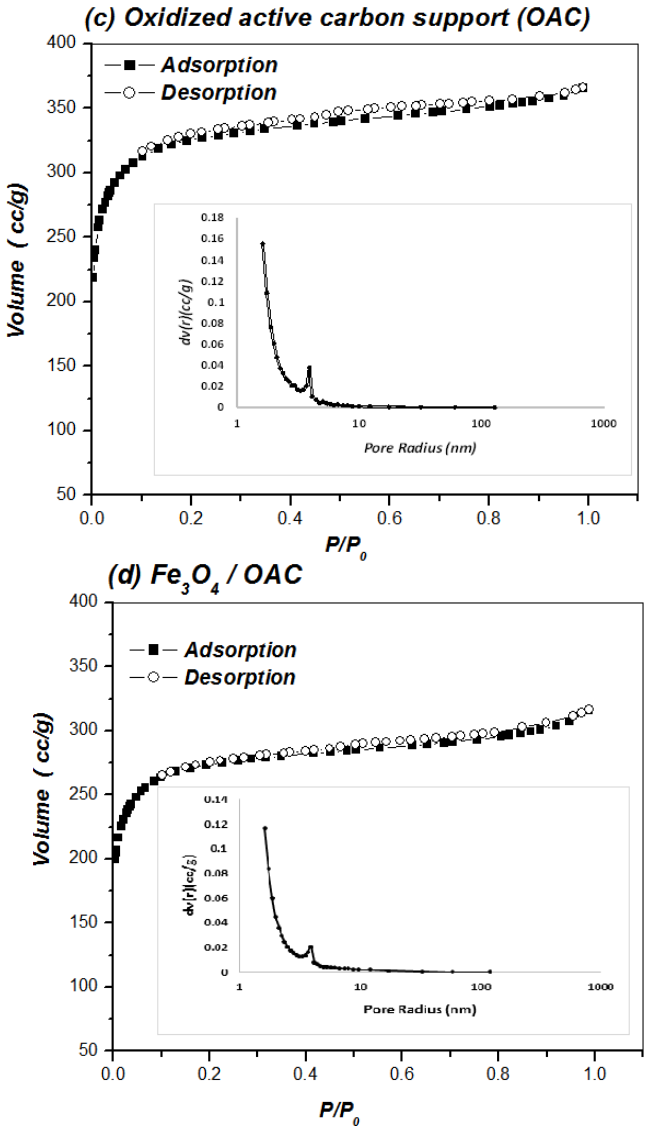

Fig.(2): N_2 adsorption-desorption isotherms and pore size distribution curves

3.1.3.Scanning electron microscope (SEM):

Scanning electron micrographs of Fe_3O_4 /AC and Fe_3O_4 /OAC are shown in Fig. (3). From this figure, it was found that the surface texture and porosity of the sample were more developed in the oxidized active carbon than in the active carbon. The availability of pores and internal surface is requisite for an effective adsorbent.

(a)

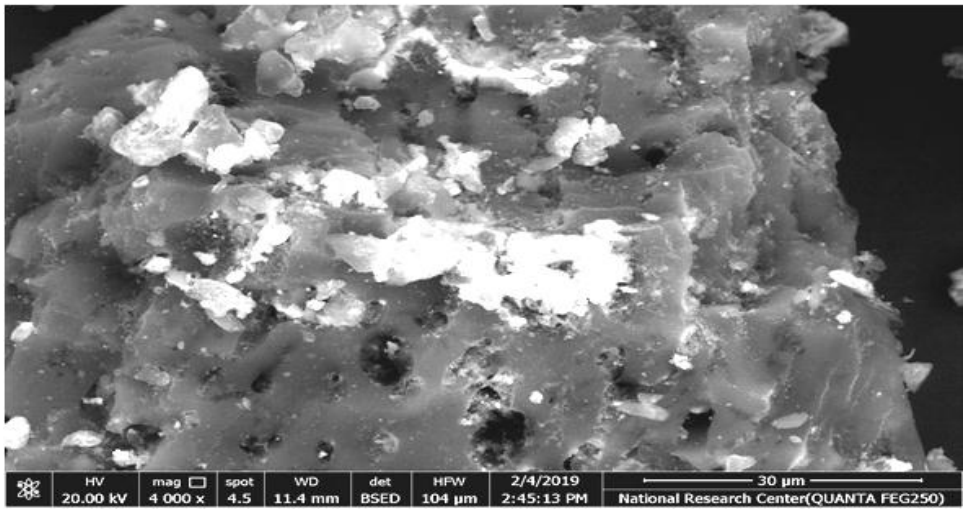

(b)

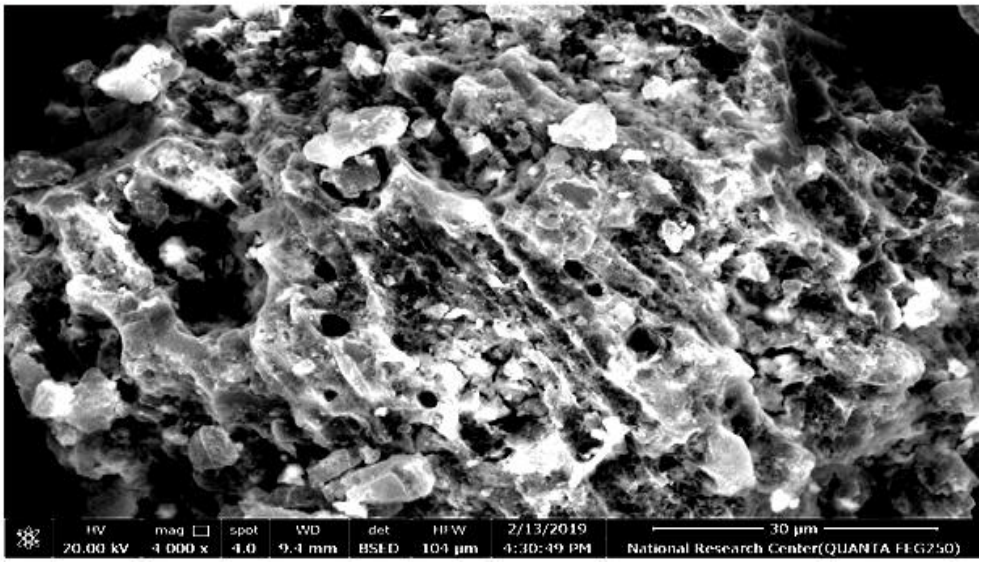

Fig.(3). SEM image of (a)Fe_3O_4/AC and (b) Fe_3O_4/OAC

3.1.4.Vibrating sample magnetometer (VSM) techniques.

The saturation magnetizations were determined by vibrating sample magnetometer (VSM) ***[Liu et al.,2010]*** as shown in Figure (4).

It was evident that as particle size is decreased; the amount of exchange-coupled spins resisting spontaneous magnetic reorientation is decreased, tending towards superparamagnetization. Obviously, the decrease of magnetite particle size led to enhanced superparamagnetic behavior.

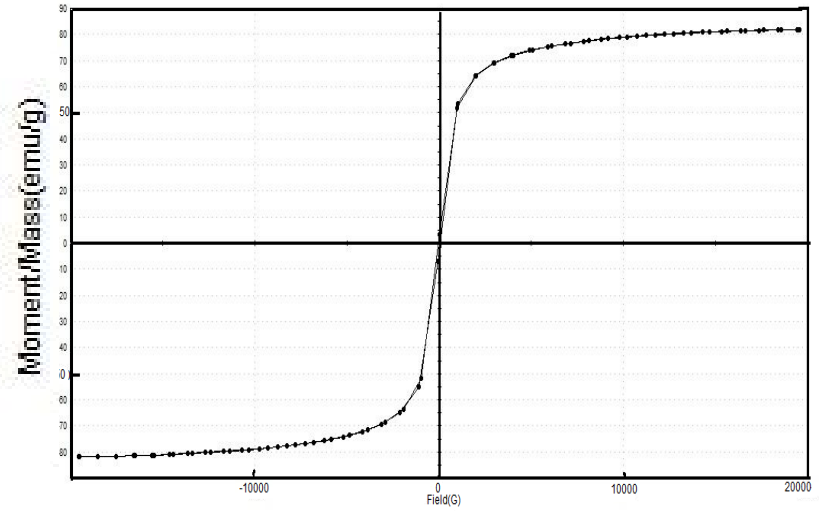

Fig.(4) The absence of hysteresis implies superparamagnetism

It is well known that magnetite particles with size less than 30 nm have a large surface area and exhibit superparamagnetic properties that make them prone to magnetic fields and they do not become permanently magnetized without an external magnetic field to support them ***[Beyaz et al.,2009]***.

3.2.Metal Removal Experiments:

3.2.1. Selection of the best ratio of magnetite loaded on support for adsorption of Cu(II) ions :

To select the best ratio of magnetite loaded on support for adsorption of Cu(II) ions the following comparisons should be checked:

- Different ratios of magnetite (Fe_3O_4) loaded on active carbon (AC) support.
- Magnetite loaded on the surface of active carbon support (Fe_3O_4/AC) and the magnetite loaded on the surface of oxidized active carbon support (Fe_3O_4/OAC).

3.2.1.1.Comparison between different ratios of magnetite (Fe_3O_4) loaded on active carbon (AC) support:

The comparison between different ratios of magnetite loaded on the surface of active carbon (AC) support was shown in Fig. (5), where the reaction was carried out by 1.0 g/l of 30 % , 15% and 7.5% Fe_3O_4/AC, respectively and the initial Cu (II) concentration was 100 mg/l with pH of the solution equal 4.8 at room temperature for 30min.

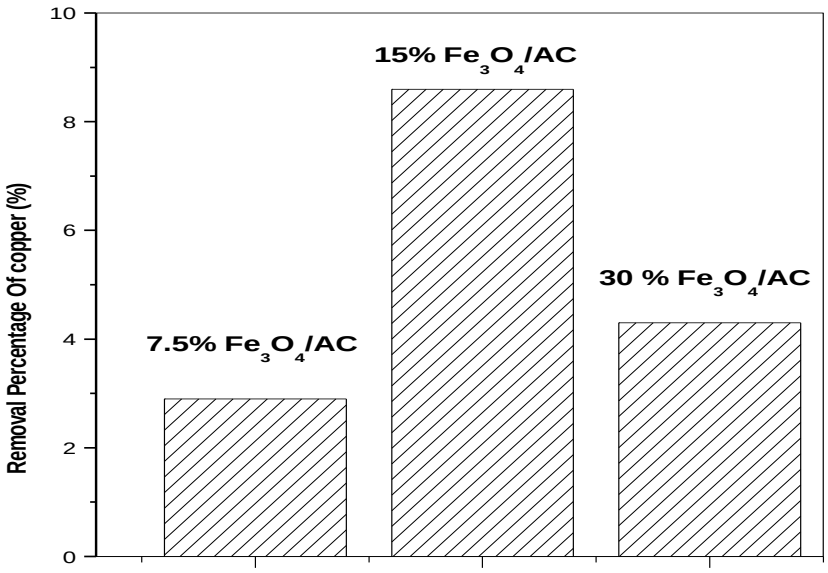

Fig.(5):The effect of different ratios of magnetite loaded on the surface of the active carbon (AC) on removal percentage of Cu(II) ions.

It was found that the removal percentage of Cu(II) was increased from 2.9% to 8.6 % by increasing the ratio of the magnetite on the active carbon support from 7.5% Fe_3O_4/AC to 15% Fe_3O_4/AC. This is due to the increasing of active sites of magnetite which was dispersed on the surface of the AC support which has highly surface area. However, when further increase of the ratio of magnetite on the surface of the AC support from 15% Fe_3O_4/AC to 30% Fe_3O_4/AC the removal percentage of Cu(II) was decreased from 8.6% to 4.3%, presumably due to probable to aggregation of magnetite particles on the surface leading to the decrease of the number of the available sorption active sites. Thus, the adsorption capacity and the removal percentage of Cu(II) was decreased.

Therefore 15% Fe_3O_4/AC was considered to be a suitable ratio of magnetite supported on active carbon for the adsorption of Cu(II).

3.2.1.2. Comparison between the adsorption capacity of magnetite loaded on the surface of active carbon support (Fe_3O_4/AC) and the magnetite loaded on the surface of oxidized active carbon support (Fe_3O_4/OAC):

Active carbon (AC) support was oxidized by HNO_3 acid to obtain oxidized active carbon (OAC) support. 15% Fe_3O_4/AC was selected for the comparison with 15% Fe_3O_4/OAC. The results are illustrated in Fig. (6).

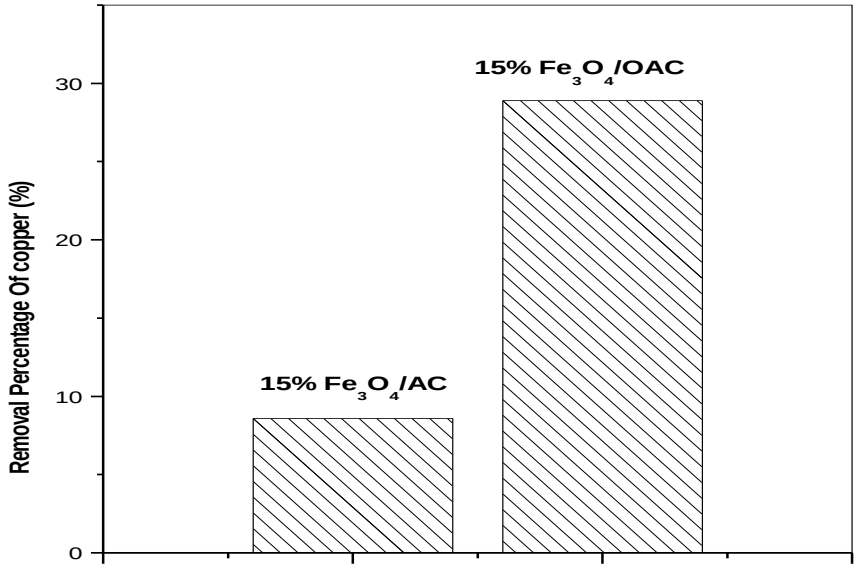

Fig.(6).Comparing between 15% Fe_3O_4/AC with 15% Fe_3O_4/ OAC

From figure (6), it can be seen that the removal percentage of Cu(II) was increased from 8.6% to 28.9 % at 30 min, when the adsorption was carried out by 1.0 g/l of 15% Fe_3O_4/AC and 15% Fe_3O_4/OAC , the initial Cu (II) concentration was 100 mg/l and the pH of the solution equal 4.8 at room temperature. This is due to the fact that, when AC were chemically oxidized by concentrated HNO_3 to form oxidized active carbon (OAC), the oxidation process allowed the implantation of various oxygen functionalities such as carbonyl, carboxylic and hydroxyl groups, onto the surface of (AC) leading to increase the removal percentage of Cu(II) ions ***[Si-Yong Gu et. al., 2019].*** Recalling the characterization results by SEM in Fig (3), the treatment of (AC) by HNO_3 could lead to increased porosity, which dictated the selection of the 15% Fe_3O_4/OAC sample for this study.

3.2.2. The effect of contact time on removal percentage of Cu(II) by 15%Fe_3O_4/OAC:

The effect of the variations in the percentage of removal of Cu(II) with contact time was shown in Fig. (7). The adsorption was performed by 1.0 g/l of 15% Fe_3O_4/OAC when the initial Cu(II) concentration was 100 mg/l and the pH of the solution equals to 4.8 at room temperature.

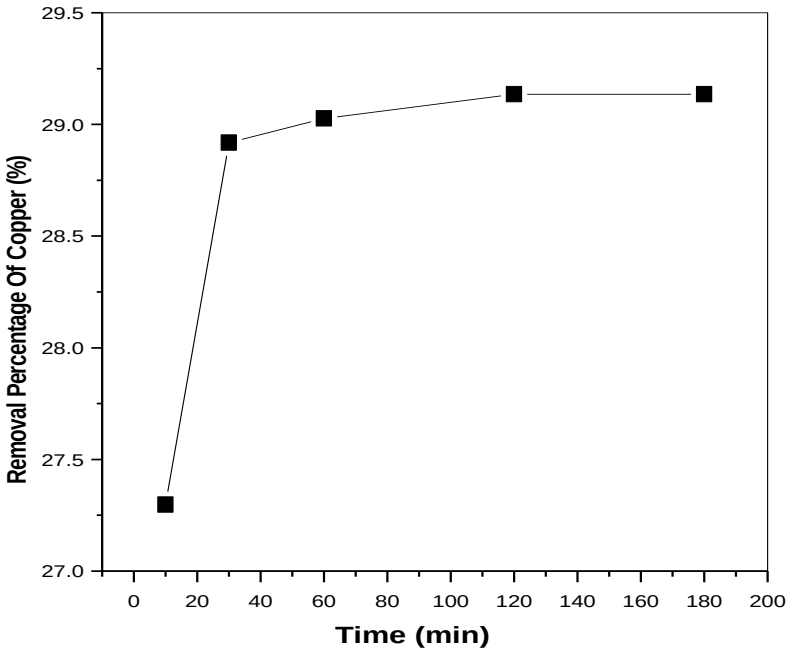

Fig.(7):The effect of contact time on the removal percentage of Cu (II) ions by 1.0 g/l of 15% Fe_3O_4/OAC when initial Cu (II) concentration was 100 mg/l and the pH of the solution was 4.8 at room temperature.

From this Fig. 7, it is observed that the removal percentages of Cu (II) are increased gradually from 27.29 % to 29.13 % by increasing the contact time from 10 to 180 minute. The removal efficiency of Cu(II) has shown a fast rate of adsorption during the first 30 minute of the adsorbate-adsorbent contact and after that the rate of removal becomes almost insignificant due to a quick exhaustion of the adsorption sites. The equilibrium reached at 30 min. which was taken as the optimal contact time for the subsequent experiments.

3.2.3.Effect of pH of the solution on the adsorption of Cu(II):

The effect of pH on the adsorption of Cu(II) by 15% Fe_3O_4/OAC nanoparticles was studied by varying the pH between 2.0 and 5.2 since at pH more than 5.2 the copper ion may be precipitated as $Cu(OH)_2$. The adsorption was carried out for 30 min. when the initial concentration of Cu(II) was 100 mg/l,the weight of 15% Fe_3O_4/OAC nanoparticles was 1.0 g/l.

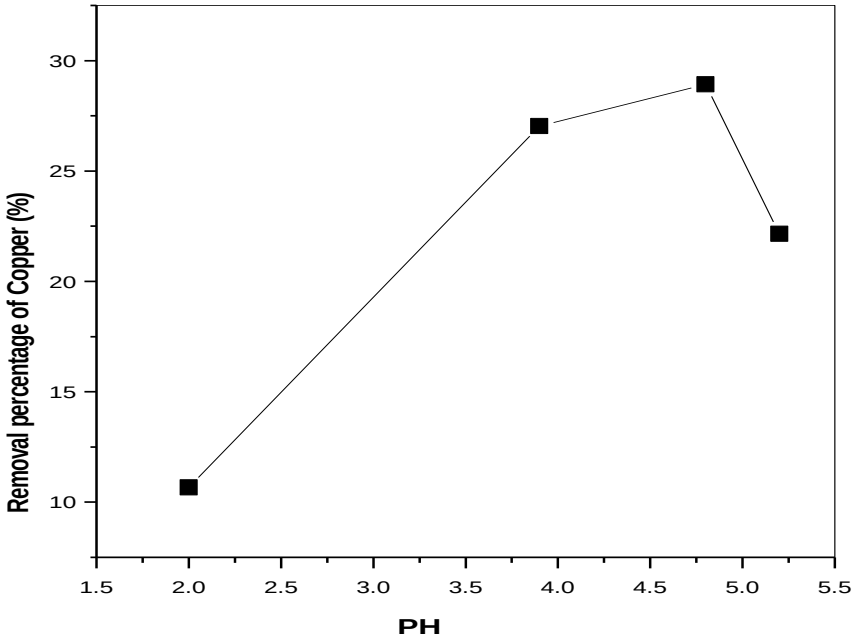

Fig.(8):The effect of the variation of pH value on the removal percentage of copper by 1.0 g/l of 15% Fe_3O_4/OAC when the contact time 30 min. and the initial Cu (II) concentration was 100 mg/l at room temperature.

As shown in Fig. (8) , the removal percentage of Cu(II) was increased from 10.6% to 28.9% with increasing the pH of the solution from 2.0 to 4.8 and it was decreased to 22.1% with further increase in the pH of the solution to 5.2. The removal percentage of Cu(II) decreased at highly acidic conditions is probably due to the presence of high concentration of H^+ ions on the adsorbent surface, competing with Cu(II) for adsorption sites. So, the maximum removal of Cu(II) was achieved at pH 4.8.

3.2.4. The effect of weight of adsorbent on the adsorption of Cu(II):

The determination of the optimal weight of adsorbent is another main parameter in the removal percentage of Cu(II). The effect of different weights (catalyst doses) of 15% Fe_3O_4/OAC was studied in a series of experiments with catalyst doses ranging between 1.0 and 10.0 g/l, the reaction was carried out when the initial concentration of Cu(II) was 100 mg/l and the pH of the solution was 4.8 at room temperature for 30 minute.

Figure (9) shows that the percentage of removal of Cu(II) was increased from 28.9% to 64.7% by increasing the adsorbent dosage from 1.0 g/l to attain maximum at 10.0 g/l because of the increase in the weight of adsorbent, the number of the available active sorption sites increases, leading to a detectable increase in the adsorption capacity with

considerable removal percentage of Cu(II). Therefore, the weight of adsorbent 10.0g/l was selected as the optimum weight.

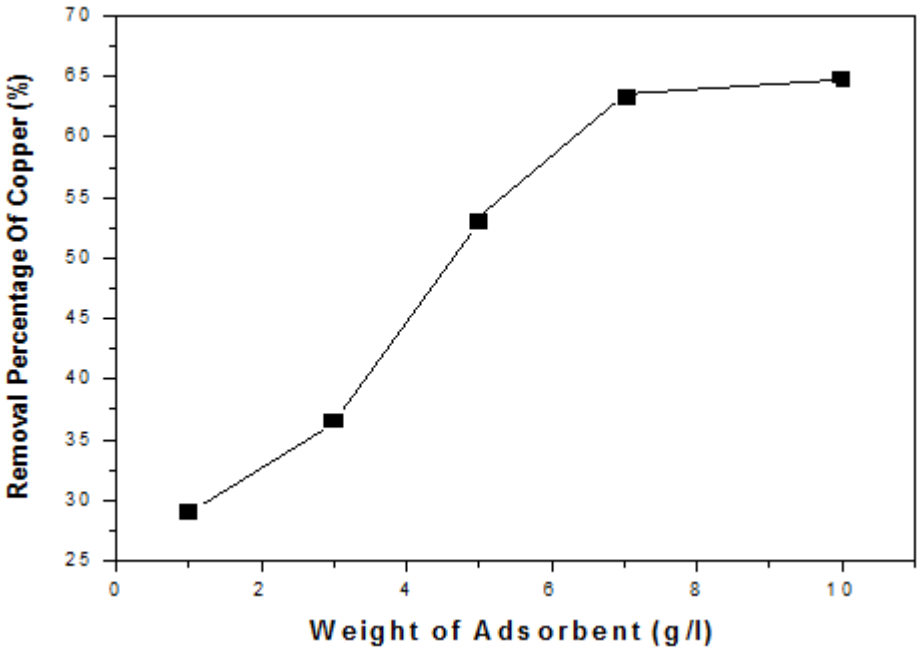

Fig.(9): The effect of variation of the weight of adsorbent on the removal percentage of copper when the initial Cu(II) concentration was 100mg/l , the contact time 30 min. and the pH of the solution was 4.8 at room temperature.

3.2.5. The effect of the initial concentration of copper on the adsorption of Cu(II):

The effect of variation of the initial concentration of copper on its removal was studied at different initial concentrations ranging from 25 to 500 mg/l, when the weight of adsorbent was 10.0 g/l, and the pH of the solution was 4.8 at room temperature at 30 min. The results are graphically repressed in Fig. (10).

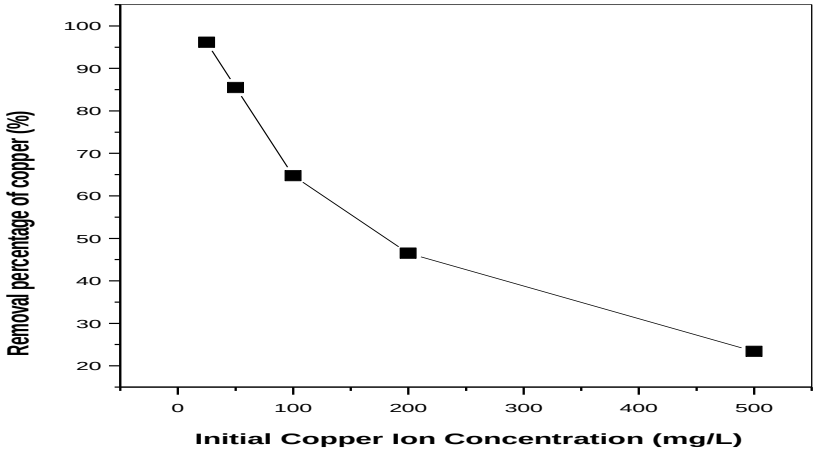

Fig.(10): The effect of variation of the initial copper concentration on the removal percentage of Cu(II) by 10.0 g/l of 15% Fe_3O_4/OAC when the contact time 30 min. , pH of solution was 4.8 at room temperature.

From this figure, it is shown that the adsorption decreases gradually from 96.15 % to 23.4% with increasing initial copper concentration from 25 to 500 mg/l. This is due to the sufficient adsorption sites available at lower initial concentration of Cu(II), but at higher initial concentrations the adsorption capacity and removal percentage of Cu(II) ions decreased due to the saturation of active sites of adsorbent and the initial concentrations of Cu(II) are greater than adsorption sites Therefore, no more adsorption of Cu(II) ions can be accompanied with increasing the initial concentration. Therefore, the availability of active sites of adsorbent is low at higher concentration of copper eventually decreasing the adsorption capacity and removal percentage of Cu(II) ions.

3.2.6. Comparison between the removal percentage of Cu(II) by unsupported Fe_3O_4, (OAC) support and 15%Fe_3O_4 supported on OAC:

Initially, the experiments was carried out when the initial concentration of Cu(II) was 25 mg/l, the pH of the solution was 4.8 at room temperature and the weight of 15% Fe_3O_4/OAC was 10.0 g/l and it was found that the removal percentage of Cu(II) was reached to 96.15%. However, when the experiment was carried out at the same condition by unsupported Fe_3O_4 and by the support only (OAC) without Fe_3O_4, it was found that the removal percentage of Cu(II) was decreased to 53.9% and 81.5%, respectively as shown in Fig.(11).

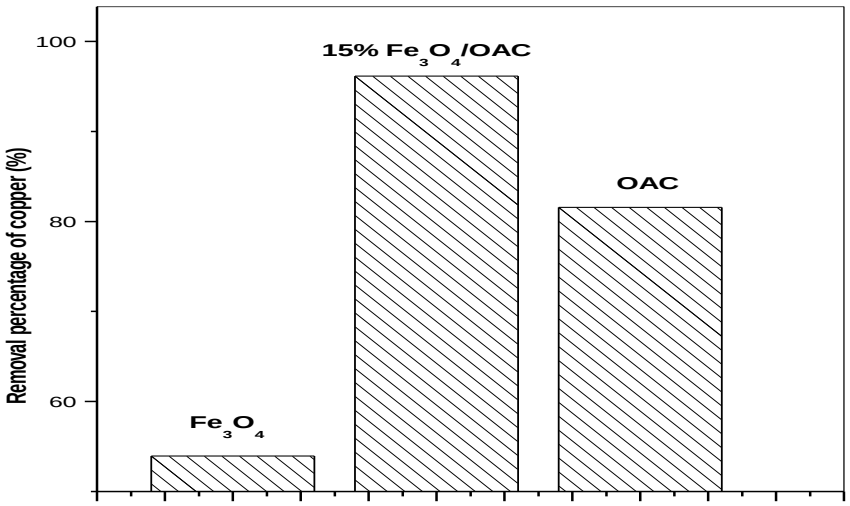

Fig.(11):Comparison between the removal percentage of Cu(II) by unsupported Fe_3O_4 , (OAC) and 15%Fe_3O_4 / OAC.

3.3. Adsorption Isotherms:

Langmuir and Freundlich isotherms for the adsorption of Cu(II) on 15% Fe_3O_4/OAC are shown in Figs. (12) and (13) respectively,. The values of the equilibrium parameters of both models, K_L, q_{max}, K_F and n, together with the corresponding regression coefficient (R^2) were computed and provided in Table (1). The Langmuir model represents a much better fit for the experimental equilibrium adsorption data of Cu(II) adsorption on the surface than Freundlich model as evidenced by relatively higher value of R^2 . This result indicated that monolayer adsorption of Cu(II) takes place on well-defined energetically equal sites and there is no subsequent interaction between the adsorbed Cu(II) molecules.

Table (1):

Parameters of Langmuir and Freundlich isotherms

Langmuir isotherm			Freundlich isotherm		
q_{max}(mg/l)	K_L(L/mg)	R^2	n	K_F	R^2
10.3018	0.0703	0.9987	3.893	2.3855	0.99256

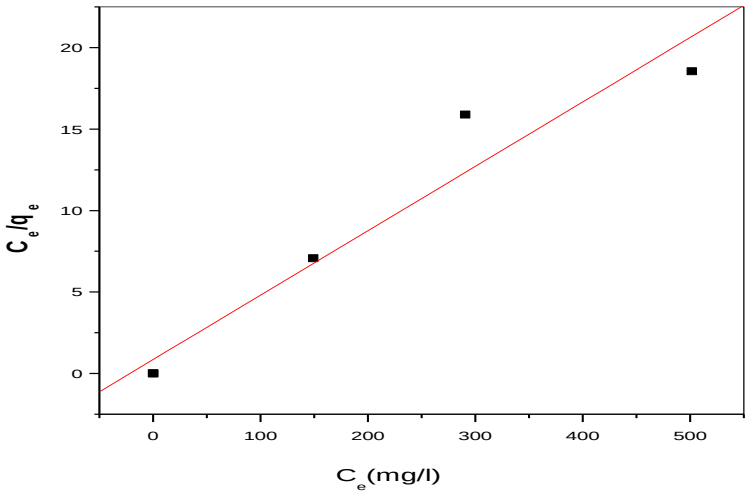

Fig.(12)Langmuir isotherm plot for adsorption of Cu(II) on 15% Fe_3O_4/OAC.

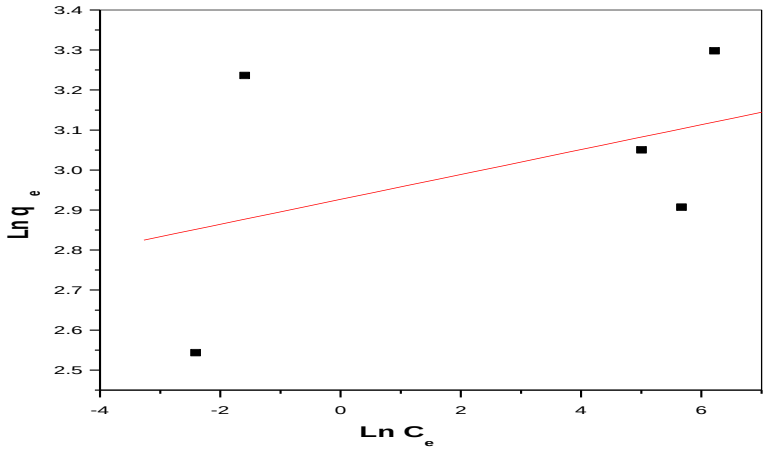

Fig.(13)Freundlich isotherm plot for adsorption of Cu(II) on 15% Fe_3O_4/OAC.

3.4. Adsorption kinetics:

Adsorption kinetics was investigated for better understanding of the mechanism of adsorption. In the present study, the adsorption data of Cu (II) at different time intervals were analyzed by the pseudo-first-order kinetic model (Eq. (1)) and pseudo-second-order kinetic model (Eq. (2) .

$$ln\,(q_e - q_t) = ln\,q_e - k_1\,t \qquad (1)$$

$$t/q_t = 1/k_2\,(q_e)^2 - t/q_e \qquad (2)$$

Where k_1 (min $^{-1}$) and k_2 (g/mg/min) are the equilibrium rate constants of pseudo-first- and pseudo-second-order rate equation, respectively.

From fig.(14) we can see the pseudo-first-order model did not fit well with the kinetics data as was evidenced from the low value of the regression coefficient (R^2 = 0.91531).

On the other hand, the good linear plot of t/q_t versus t based on pseudo-second order kinetic model, as shown in Fig (15), with extremely high regression coefficient is near to unity (R^2 = 1)

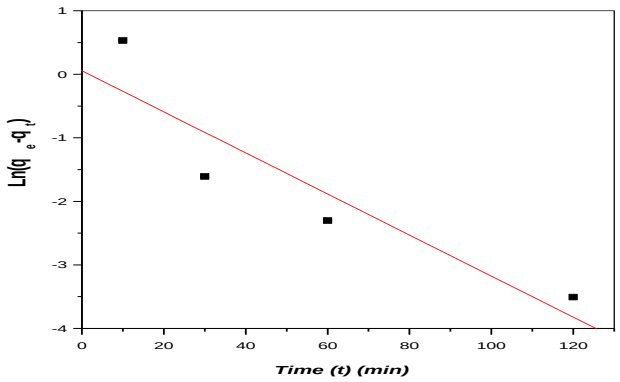

Fig.(14): Pseudo-first-order linear plots for adsorption of Cu(II) on 15% Fe_3O_4/OAC.

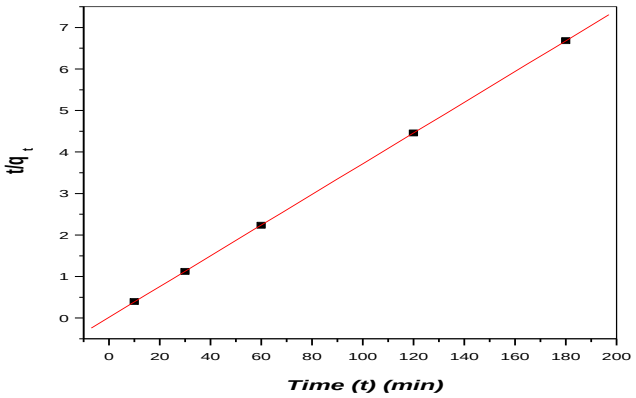

Fig.(15): Pseudo-second-order linear plots for adsorption of Cu(II) on 15% Fe_3O_4/OAC.

4.Conclusions:

The results showed that 15%Fe_3O_4/OAC nanoparticles prepared by co-precipitation method is more active than 15%Fe_3O_4/AC for removal of Cu(II) ions from aqueous solutions. The equilibrium was achieved practically in 30 min. and the percentage removal of copper was 96.15%. Langmuir model is found to be in a good agreement with experimental data on adaptive behavior of Cu(II) ions by 15% Fe_3O_4/OAC and considered as a useful adsorbent for the treatment of wastewater containing copper. The kinetic study indicated that the adsorption of copper followed the second-order adsorption.

5. Reference

Awual M.R., Ismael M., Yaita T., El-Safty S.A., Shiwaku H., Okamoto Y., Suzuki S., Trace copper (II) ions detection and removal from water using novel ligand modified composite adsorbent, Chem. Eng. J. 222 ,67–76(2013).

Babak Kakavandi, Roshanak Rezaei Kalantary, Mahdi Farzadkia A.H. Mahvi, A. Esrafili, A. Azari, A.R. Yari, A.B. Javid, Enhanced chromium (VI) removal using activated carbon modified by zero valent iron and silver bimetallic nanoparticles J. Environ. Health Sci. Eng. 12, 1–10 (2014)

Babel S. and Kurniawan T.A., Low-cost adsorbents for heavy metals uptake from contaminated water: a review, J. Hazard. Mater. 97 ,219–243(2003).

Beyaz S., Kockar H. and Tanrisever T., Simple synthesis of superparamagnetic magnetite nanoparticles and ion effect on magnetic fluids, Journal of Optoelectronics and Advanced Materials, **1**, 447 - 450 (2009).

Binu P Jacob, Ashok Kumar, Pant R. P. , Sukhvir Singh and Mohammed E. M., Influence of preparation method on structural and magnetic properties of nickel ferrite nanoparticles, Indian Academy of Sciences, **34**(7), 1345–1350(2011).

Dimitrov, D., Interactions of antibody-conjugated nanoparticles with biological surfaces. Colloids Surf A,.282–283,8-10, (2006).

Ertugay N., and Malkoc E., Adsorption isotherm, kinetic, and thermodynamic studies for methylene blue from aqueous solution by needles of Pinussylvestris L. Pol , Environ Stud., **23**,1995–2006(2014).

Friedrich, KA. Henglein, F., Stimming, U., Unkauf, W., Investigation of Pt particles on gold substrates by IR spectroscopy particle structure and catalytic activity. Colloids Surf A,134, 193–206, (1998).

Fu F. and Wang Q., Removal of heavy metal ions from wastewaters: a review, J. Environ.Manag. 92 ,407–418(2011).

Gupta, AK., Gupta, M., Synthesis and surface engineering of iron oxide nanoparticles for biomedical applications. Biomaterials 26, 3995–402, (2005).

Hameed B.H., Mahmoud D.K., Ahmad A.L., Equilibrium modeling and kinetic studies on the adsorption of basic dye by a low-cost adsorbent: Coconut (Cocos nucifera) bunch waste,Journal of Hazardous Materials, **158**, 65-72 (2008**).**

Huang, SH., Liao, MH., Chen, DH., Direct binding and characterization of lipase onto magnetic nanoparticles. Biotechnology Prog, 19, 1095–100, (2003).

Ihsanullah A., Abbas A.M., Al-Amer T.,.Laoui M.J, Al-Marri M.S., Nasser M., AtiehKhraisheh M.A., Heavy metal removal from aqueous solution by advanced carbon nanotubes: critical review of adsorption applications, Sep. Purif. Technol. 157 ,141–161(2016).

Liu C., Bai R., San Ly Q., Selective removal of copper and lead ions by diethylenetriamine-functionalized adsorbent: behaviors and mechanisms, Water Res. 42 ,1511–1522(2008).

Liu X., Guo Y. and Weng Y., Direct synthesis of mesoporous Fe_3O_4 through citric acid-assisted solid thermal decomposition. J. Mater. Sci. , **45**, 906–910 (2010**).**

Long Giang Bach, Kwon Taek Lim , Bui Thi Phuong Quynh , Le Thi Hong Nhan and Trinh Duy Nguyen, A Facile Method for Preparation and Characterization of Fe_3O_4 Magnetic Nanoparticles, Journal of Materials Science & Surface Engineering, **4**(4), 407-409 (2016).

Lua A.C. and Yang T., Effect of activation temperature on the textural and chemical properties of potassium hydroxide activated carbon prepared frompistachio-nut shell, J. Colloid Interface Sci. 274 ,594–601(2004).

Luo X., Lei X., Cai N., Xie X., Xue Y., Yu F., Removal of heavymetal ions fromwater by magnetic cellulose-based beads with embedded chemically modified magnetite nanoparticles and activated carbon, ACS Sustain. Chem. Eng. 4 ,3960–3969 (2016).

Ming Hua, Shujuan Zhang, Bingcai Pan, Weiming Zhang, Lu Lv, Quanxing Zhang, Heavy metal removal from water/wastewater by nanosized metal oxides: A review. Journal of Hazardous Materials 211–212 ,317–331(2012).

Muhammad S, Shah M.T., Khan S., Health risk assessment of heavy metals and their source apportionment in drinking water of Kohistan region, northern Pakistan, Microchem. J. 98 ,334–343(2011).

Nikhat Neyaz1 and Weqar A. Siddiqui, Removal of Cu (II) by Modified Magnetite Nanocomposite as a Nanosorbent . International Journal of Science and Research, Volume 4 Issue 2, (2015).

Perić J., Trgo M., VukojevićMedvidović N., Removal of zinc, copper and lead by natural zeolite—a comparison of adsorption isotherms, Water Res. 38 ,1893–1899(2004).

Prahas D., Kartika Y., Indraswati N., Ismadji S., Activated carbon from jackfruitpeel waste by H3PO4 chemical activation: pore structure and surfacechemistry characterization, Chem. Eng. J. 140 ,32–42(2008).

Randhaw, N.S., Dwivedi, D., Prajapati, S., Jana, R.K., Application of manganese nodules leaching residue for adsorption of nickel(II) ions from aqueous solution. Int. Env. Sci. Tech. 12 (3), 857–864(2015)**.**

Roto,Yusran, Yusran and Agus, Kuncaka, Magnetic adsorbent of Fe_3O_4-SiO_2 core-shell nanoparticles modified with thiol group for chloroauric ion adsorption, Applied Surface Science, **377**(30), 30-36 (2016).

SekarM.,Sakthi V. and Rengaraj S., Kinetics and equilibrium adsorption study of lead(II) onto activated carbon prepared from coconut shell,Journal of Colloid and Interface Science,**279**(2), 307-313(2004).

Shalini Rajput, Charles U. Pittman Jr. and Dinesh Mohan **,** Magnetic magnetite (Fe_3O_4) nanoparticle synthesis and applications for lead (Pb^{2+}) and chromium (Cr^{6+}) removal from water, Journal of Colloid and Interface Science, **468**, 334–346(2016).

Shamsan S. Obaida, Gaikwada D. K., Sayyedc M. I., Khader AL-Rashdia and Pawar P. P., Heavy metal ions removal from waste water bythe natural zeolites, Materials Today Proceedings, **5**, 17930–17934 (2018).

Si-Yong Gu, Chien-TeHsiehb, Yasser Ashraf Gandomi, Zhi-Feng Yang, Lingyun Li, Chun-Chieh Fu, Ruey-Shin Juang, Functionalization of activated carbons with magnetic Iron oxide nanoparticles for removal of copper ions from aqueous solution. Journal of Molecular Liquids 277 , 499–505(2019).

Srivastava N.K. and Majumder C.B., Novel biofiltration methods for the treatment of heavy metals from industrial wastewater, J. Hazard. Mater. 151 ,1–8(2008).

Wang S. and Lu G.Q., Effects of oxide promoters on metal dispersion andmetal-Support interactions in Ni catalysts supported on activated carbon, Ind.Eng. Chem. Res. 36 ,5103–5109(1997).

Wu HB, Wei S, Zhang L, Xu R, Hng HH, Lou XWD. Embedding sulfur in MOF- 681 derived microporous carbon polyhedrons for lithium–sulfur batteries. Chem–A 682 Euro J;19:10804–8,
(2013).

الملخص باللغة العربية

ازالة ايونات النحاس من مياه الصرف باستخدام اكسيد الحديد المغناطيسي المحمل على الكربون النشط والكربون النشط المؤكسد

آيه صبرى محمود [١] و ناديه عبد الحكيم يوسف [١] و احمد اسامة ابو النجا [٢] و محمد محمد سليم [٣]

١. قسم الكيمياء ،كليه البنات –جامعة عين شمس.
٢. معهد بحوث البترول
٣. المركز القومي للبحوث

تم تحضير اكسيد الحديد المغناطيسي Fe_3O_4 بواسطة طريقة الترسيب المشترك وتحميله على الكربون النشط (Fe_3O_4 / AC) والكربون النشط المؤكسد (Fe_3O_4/OAC) ثم توصيفهم بحيود الأشعة السينية (XRD) و المجهر الإلكترونى الماسح (SEM) ، وقياسات مساحة السطح (BET) وتقنيات مقياس الاهتزاز المغناطيسي للعينة (VSM). تم استخدام Fe_3O_4 / AC و Fe_3O_4 / OAC كمواد مازة لإزالة أيونات النحاس (II) من مياه الصرف الصناعى .درست عوامل الامتزاز مثل وقت التجربة ، ودرجة الحموضة في المحلول ، وجرعة المادة المازة والتركيز الأولي لأيونات الـ Cu(II) . تم إجراء دراسة لظروف التشغيل المثالى للعملية وظهر أن نسبة إزالة أيونات Cu (II) قد وصلت إلى ٩٦.١٥٪ خلال ٣٠ دقيقة. ووجد انه باستخدام Fe_3O_4 / OAC كمواد مازة لإزالة أيونات النحاس (II) من مياه الصرف الصناعى تتفق مع نموذج لانجمير وذلك طبقا لمقارنة (regression coefficient-R) لكل من نموذج فرويندليش و نموذج لانجمير. كما تمت دراسة الكيمياء الحركية للتفاعل وتم الوصول الى انه يسلك الرتبة الثانية الزائفة من الكيمياءالحركية